Identification of Genes During the Reprogramming of Fibroblast using Bioinformatics Analysis

Peng Wu
Guangdong General Hospital: Guangdong Provincial People's Hospital
Xiyalatu Sai
Guangdong General Hospital: Guangdong Provincial People's Hospital
Xiaoying Tang
Guangdong General Hospital: Guangdong Provincial People's Hospital
Huiming Guo
Guangdong General Hospital: Guangdong Provincial People's Hospital
Huanlei Huang
Guangdong General Hospital: Guangdong Provincial People's Hospital
Moussa Ide Nasser (nassermoussa83@yahoo.com)
Guangdong General Hospital: Guangdong Provincial People's Hospital https://orcid.org/0000-0002-2670-6496
Ping Zhu
Guangdong General Hospital: Guangdong Provincial People's Hospital

Research

Keywords: Fibroblast, iPSCs cells, differentially expressed gene, regulatory networks

Posted Date: June 29th, 2021

DOI: https://doi.org/10.21203/rs.3.rs-632796/v1

Abstract

Bioinformatics method was used to screen Human induced pluripotent stem cells reprogrammed by Human Fibroblasts (FBs). The reprogramming efficiency was explored by difference expressed genes (DEGs) before and after the expression of hiPSCs. Likewise, microarray datasets GSE34309, GSE43996, and GSE56805 datasets were downloaded from Gene Expression Omnibus (GEO) and GEO2R to screen the differentially expressed DEGs. Further, Gene Ontology (GO) and KEGG (Kyoto Encyclopedia of Genes and Genomes (KEGG) signaling pathways were analyzed by David database. Likewise, to explore the correlation between DEGs, and the STRING database software was used to construct the protein-protein internet (PPI), and the Cytoscape_v3.7.2 Cytohubba plug-in was used to screen out the core genes. A total of 622 DEGs were identified, including 344 up regulated genes and 278 down-regulated genes. DEGs were mainly concentrated in the cell cycle and PI3K-Akt signaling pathway. Among the ten core genes screened, CDK1, IL6, EGFR, FN1, CDH1, SOX2, BRCA1, EZH2, CD44, and CCNB1 were most significant in the reprogramming of FBs into iPSCs. Regardless underline the differential of those gene expression profiles and regulatory network during FBs reprogramming could provide a theoretical basis for efficient reprogramming.

Introduction

Induced pluripotent stem cells (iPSCs) are a class of cells with an infinite capacity for self-renewal, a healthy karyotype, and the potential to discriminate between endoderm, mesoderm, and ectoderm [1, 2]. Chemical reprogramming of cells in mammals was first recorded when 5-azacytidine-like DNA turned fibroblast (FBs) into cardiomyocytes. While studies progressed, chemicals were discovered after the other to transition to cell destiny [3]. The reprogramming strategy of iPSCs proposed by Takahashi et al.[4] made a significant breakthrough in the transfer of fate between somatic cells and pluripotent cells, including converting FBs to iPSCs by the four transcription factors (TFs) identified as OCT4, SOX2, KLF4a, and c-Myc (OSKM).

At present, iPSCs have replaced the likelihood of renewable and non-renewable organizations, like the heart, pancreas, and brain tissue [5–7]. Also, studies have reported that iPSCs can improve cardiac function after myocardial infarction in non-human primates and functional motor disorders in Parkinson's disease; nevertheless, these confirm the strong potential of iPSCs as cell replacement therapies [7, 8]. Simultaneously, somatic-derived iPSCs face fewer ethical problems than embryonic stem cells (ESCs). On this basis, patient/disease-specific functional cells derived from iPSCs help build individualized disease models, facilitate drug discovery, and establishing specific treatment protocols. It also laid the foundation for the development of regenerative medicine [9–11]. However, due to the resistance of somatic cells to the reprogramming process, the experimental period was prolonged, and the reprogramming efficiency was reduced to some extent [12, 13]. Although some studies have pointed out that chemical molecules and non-coding RNAs can optimize the traditional reprogramming scheme to a certain extent and improve the reprogramming efficiency [14–16]. However, there are few reports on its potential regulatory mechanism.

Besides, during the reprogramming process of somatic cells, iPSCs can show differences and integrity at different molecular and gene levels [17]. Therefore, revealing the gene expression changes and potential functions of cell lines before and after reprogramming is of key significance for the subsequent optimization of the reprogramming scheme, showing the regulatory mechanism and improving reprogramming efficiency.

This study analyzed the microarray data of GSE34309, GSE43996, and GSE56805 and screened the differentially expressed genes (DEGs) during reprogramming, among which 344 up regulated genes and 278 down-regulated genes were identified. The GO annotation and KEGG signal pathway enrichment analysis were performed on DEGs based on the online website of David, and the PPI network was constructed by using the STRING database and Cytoscape software and 10 core genes were screened out. They were CDK1, IL6, EGFR, FN1, CDH1, SOX2, BRCA1, EZH2, CD44, and CCNB1. Our study reveals the differential gene expression profiles and regulatory networks in the reprogramming process of FBS, which is expected to provide a basis for improving the reprogramming efficiency.

Results

DEGs screening

Three microarray datasets, including GSE34309, GSE43996, and GSE56805, are represented by the limma packet algorithm in the R language of Geo2R's online analysis tool for background correction and data normalization. Adj. $P < 0.05$ and $|logFC| \geq 2.0$ were set as a threshold, the GSE34309 dataset was screened, and 1366 DEGs were obtained, including 606 up regulated genes and 760 down-regulated genes. Using a same method, 1390 DEGs were obtained from the GSE43996 dataset, including 638 up regulated genes and 752 down-regulated genes, and 2041 DEGs were screened, including 1257 up regulated genes and 784 down-regulated genes. The sample data of the three datasets are shown in Figure 1, also known as the Volcano Map. Then, the Venn diagram is plotted to obtain the intersection of DEGs (Figure 2). Finally, 622 DEGs were overlapped in the three data series, with 344 genes up regulated and 278 genes down regulated. Clustering heat maps of 622 DEGs in the three microarrays were made by R X64 3.6.2 software (Figure 3).

GO function annotation analysis of DEGs

To better understand DEGs' position, the GO feature annotation analysis of DEGs was carried out using the David online method, including CC, MF, and BP. In conjunction with $P < 0.05$, the GO analysis of the most important top 30 was chosen (Table 2). We observed that the following functional groups, including extracellular matrix, DNA replication, mitosis, cell cycle, protein binding, etc., were mainly enriched with these DEGs (Figure 4).

KEGG pathway enrichment analysis of DEGs

For the KEGG pathway enrichment study of DEGs, David's online method was used, and statistically significant pathways were chosen according to $P < 0.05$ (Table 3). We observed that these DEGs were primarily enriched in the cell cycle, replicating DNA, an association of extracellular matrix receptor, cell division, p53 signaling pathway(Figure 5).

Establish PPI network, conduct module analysis, and select HUB genes

A PPI network using the STRING database was developed to investigate the biology of these DEGs further. Of the 584 network nodes, there are 8258 edges, as seen in Figure 6. (a). The essential modules in the PPI network were subsequently evaluated, and, as seen in Figure 6, 87 nodes and 3412 edges were screened out (b). Bub1 was the most important gene in the PPI network and was primarily concentrated in the cell cycle. The top 10 core genes are screened based on the Cytohubba widget-based Degree and bulk algorithm, and sub-networks are created, as seen in (Figure 6c and d). Five common HUB genes, CDK1, EGFR, FN1, BRCA1, and CCNB1, as seen in Figure 6, were screened out, according to the Venn diagram (d).

Discussion

iPSCs are very similar to ESCs in morphology, gene and protein expression, epigenetic modification, cell proliferation, and differentiation and can differentiate into cardiomyocytes, nerve cells, liver cells, and islet cells. Importantly iPSCs can be reprogrammed from somatic cells, so there is no immune rejection. They have a wide range of applications, including personalized drug screening, gene correction, cell transplantation, and tissue engineering, making them essential in regenerative medicine research. At the same time, it avoids the ethical difficulties that ESCS faces in terms of access [18].

Although it has a decent chance of implementation, several questions still need to be addressed because transcription factors are required to use viruses as vectors during reprogramming; incorporating the virus-mediated genomic DNA gene is probable, leading to proto-oncogenes activation and tumor-forming induction[19]. Likewise, Nakagawa et al. 18059259 demonstrated that the efficacy of OSKM's reprogramming of FBs into HIPSCs was poor. Therefore, the key challenges encountered at present are improving reprogramming and reducing the usage of transcription factors. According to a previous report, we find that it can provide valuable knowledge for improving reprogramming schemes and improving reprogramming performance by disclosing the main events controlling reprogramming and the multifunctional regulatory network [20].

A total of 622 DEGs, including 344 up regulated and 278 down-regulated genes, were defined in this study from three datasets, GSE34309, GSE43996, GSE56805, utilizing online research methods for integrated bioinformatics and Geo2R. We established that these DEGs were predominantly localized in the following functional categories by GO functional annotations, including extracellular matrix, DNA replication, mitosis, cell cycle, protein binding, etc. Likewise, we discovered that these DEGs were mainly enriched by the cell cycle, DNA replication, extracellular matrix receptor interaction, cell division, p53 signaling pathway, etc., from the KEGG pathway enrichment study. The PPI network was being built using the

String database. Then, essential modules were studied in the PPI network, and Bub1 was the most fundamental gene in the PPI network, focused mainly on the cell cycle. Five HUB genes, including CDK1, EGFR, FN1, BRCA1, and CCNB1, have been screened in particular.

A significant aspect of the spindle check-up method is benzene and imidazole budding disinhibiting homolog protein 1 (BUB1). The spindle inspection performs an essential function during mitosis. It aims to ensure that genetic material replicated by cells in the mitotic chromosome phase is safe and correct after being allocated to each child cell and to prevent the occurrence of aneuploidy daughter cells. Lowering the BUb1 breast cancer cell line has been shown to avoid xenograft in immunocompromised mice, primarily attributed to decreased tumor stem cell capacity and improved susceptibility to radiotherapy[21]. Therefore, in stem cell pluripotency preservation, Bub1 is active. Likewise, Li et al. [22] found that Bub1, OCT4, Nanog, TDGF1, and other dry genes were heavily expressed and responsible for cell self-renewal and pluripotent differentiation via the discovery of gene expression profiles in ESCs. Our results were concordant with the previous findings and provided insights into the molecular mechanism.

Fibronectin (FN), one of the main fibrillary proteins, has been involved in cell-multitrophic (cell-differentiating) and cellular proliferation and differentiation. Following FN1-KO extension, the number of human infrapatellar fat pad derived stem cells was increased, but this rise was negated by FN1 cells after implantation into ECM[23]. Likewise, recent findings have found that the glucocorticoid receptor enhances the proliferative mesenchymal progenitor cell's acquisition of fibroblast matrix-derived signals such as Fn1 through and Wnt-1 and JAK-STAT, concerning their activity in the extracellular environment by other cells, and thus indirectly regulates a subset of those cells responsible for promoting tissue extracellular matrix gene expression, especially the cells[24]. Therefore in this study, we might be supposed that Fn1 is one of the major factors that enhance the reprogramming factors of FBs into iPSCs

It’s well known that in cell cycle control, especially mitosis, cyclin-dependent kinase 1 (CDK1) plays a key role. Previous studies have shown that CDK1 down regulation contributes to G2 step aggregation of HIPSCs, dry gene down regulation (OCT4, KLF4, and LIN28), and pluripotent morphology failure. Various lineage markers, linked to the separation of trophoblastic ectoderm, and spreading to other lineages, such as ectoderm, mesoderm, and endoderm, are up regulated [25]. Wang et al. [26]further revealed that CDK1 would target PDK1 directly, thereby influencing PI3K/Akt's behavior and its ERK and GSK3β effectors. Also, by controlling IPSC maturation, the CCNB1-CDK1 complex may facilitate somatic reprogramming performance since cyclin B1 may induce higher LIN28A levels, indicating that this could be a new direction to increase reprogramming efficiency and also provide a new pluripotency regulation and acquisition kinase cascade mechanism. Therefore, we might suggest that the complex CCNB1-CDK1 plays a pivotal role in regulating the cell cycle in iPSCs during reprogramming.

Brill et al. [27]found out that the EGFR family is active in pluripotent stem cell self-renewal and that widespread apoptosis has been observed in undifferentiated pluripotent stem cells treated with 10 M EGFR inhibitors, in line with previous reports[28]. Indeed, EGFR trans-membrane, which connects the cellular signal transduction with the growth, differentiation, and survival by interacting with EGF and other

growth factors (EGF) or other types of growth factors to bind with it, thereby allowing it to initiate signal transduction pathways. Thus, suppression of EGFR signaling is conducive to gene reprogramming. Therefore, large amounts of epigenetic modulation are observed to cover a broad spectrum of cardiac enhancers, the researchers noted, and how they are linked to the regulatory mechanisms involved in myocyte reprogramming [29]. Regardless we might hypothesize that knockdown of the gene EGFR during reprogramming of FBs into iPSCs could enhance the reprogramming rate.

Through studying the genomes of the 24 iPS lines, researchers found that they have the same types of derivative gene mutations (de novo) in both BRCA and non-BRCA tumor types. This evidence demonstrates that BRCA-1 fibroblast-derived iPS lines may be used to research mutation impact on gene stability and the resulting gene expression [30]. Furthermore, double knockdown experiments discovered that BRC1 works, and a DNA harm response were also shown to be needed for it. The combination of Mesenchymal to epithelial transformation is also occurring at decreased levels in BRCA-1 knockouts. Thoroughly comprehending the context-dependent expansion is a key to understanding the shape and structure of the colonies that are formed as critical in early reprogramming often establishes baseline characteristics of morphology [31]. Taken together, we suppose that inhibition of BRCA-1 could also enhance the reprogramming ratio of FBs into iPSCs.

Conclusions

In conclusion, the key aspect of this manuscript is bioinformatics methods to generate and reprogram fibroblast products in gene and regulatory network differential expression profiles. The mechanism has been illustrated under three data sets, and our data justify the overlapping of 622 DEGs, up regulating 344 genes and down regulating 278 genes. DEGs, reproduced by DNA (extracellular matrix receptor) and cell division (signalization pathway p53), are enriched throughout the cell cycle. DEGs are often supplemented with different functional classes such as the extracellular matrix, DNA reproduction, and mitosis. We find five genes that play an essential role in the reprogramming of FBs into iPSCs. Therefore open a new horizon for further researchers.

Material And Methods

Data Sources

Research and analyze genetic data sets from the national center for biotechnology information comprehensive center (https://www.ncbi.nlm.nih.gov/gds/) gene expression. We chose GSE34309, GSE43996, and GSE56805 as the data set of this study. There were 9 cases of Human FBS and 23 cases of hiPSCs. Detailed information on the data sets is listed in Table 1. Volcano maps of the three data sets were made by R X64 3.6.2 software. All data can be downloaded online for free, and the study did not involve any human or animal experiments.

Screening of differentially expressed genes

GEO2R online analytical tool (https://www.ncbi.nlm.nih.gov/geo/geo2r/) based on the R language limma packet algorithm, is applied to the analysis of FBs and hiPSCs between DEGs. Adjusted P (Adjusted P, adj P) < 0.05 and |logFC|≥2.0 were set as thresholds to screen DEGs. The heat map was made by R x64 3.6.2 software. Then, use the Venn diagram online tool (http://bioinformatics.psb.ugent.be/webtools/Venn/) three data sets to identify common DEGs.

GO annotation and KEGG pathway enrichment analysis

Database for Annotation, Visualization, and Integrated Discovery DAVID) (https://david.abcc.ncifcrf.gov/) is used in genome function annotation of online websites [18]. In this study, Gene Ontology (GO) and KEGG (Kyoto Encyclopedia of Genes and Genomes (KEGG) signaling pathway enrichment analysis were performed on DEGs using the David database. The GO annotation contains the Cellular component (CC), Molecular function (MF), and biological process (BP).Set adj.P < 0.05 as the threshold.

Build PPI network

Using the Search Tool for the Retrieval of Interacting Genes (String) online database (https://string-db.org/) to predict PPI networks, combined with a score of > 0.4 that was considered statistically significant, analysis of functional interactions between proteins may provide insights into the mechanisms involved. Cytoscape is software for network visualization and analysis and editing. It uses Cytoscape_v3.7.2 software to draw DEGS interaction and visualize and analyze the PPI network. In order to find the modules of the whole network, using The molecular complex detection (MCODE) plug-in, the criteria for selection were as follows: MCODE scores >5, degree cut-off=2, node score cut-off=0.2, Max depth=100, and K-score =2. Based on the CytoHubba plug-in, the top 10 core genes were screened, and sub networks were constructed.

Declarations

Ethics approval and consent to participate: Not applicable

Consent for publication: All authors consent

Funding: This research was funded by National Key Research and Development Program of China (2018YFA0108700, 2017YFA0105602), NSFC Projects of International Cooperation and Exchanges (81720108004), National Natural Science Foundation of China (81974019), The Research Team Project of Natural Science Foundation of Guangdong Province of China (2017A030312007). The key program of Guangzhou science research plan (201904020047). The Special Projects of Dengfeng Program of Guangdong Provincial People's Hospital DFJH201812, KJ012019119, KJ012019423.

Availability of data and material: Not Applicable

Competition of Interest: The authors have declared that no competing interests exist.

Author Contributions: Conceptualization PW, XT, XS, investigation PW, XT, XS, MIN, original draft preparation PW, XT, XS,MIN , review and editing PW, XT, XS,MIN, HG, HH, PZ, funding acquisition HH, HG, MIN, PZ.

References

1. Siller R, Sullivan GJ. **Rapid Screening of the Endodermal Differentiation Potential of Human Pluripotent Stem Cells**. *Curr Protoc Stem Cell Biol* 2017, 43:1G 7 1-1G 7 23.
2. Siller R, Naumovska E, Mathapati S, Lycke M, Greenhough S, Sullivan GJ. Development of a rapid screen for the endodermal differentiation potential of human pluripotent stem cell lines. Sci Rep. 2016;6:37178.
3. Taylor SM, Jones PA. Multiple new phenotypes induced in 10T1/2 and 3T3 cells treated with 5-azacytidine. Cell. 1979;17(4):771–9.
4. Takahashi K, Yamanaka S. Induction of pluripotent stem cells from mouse embryonic and adult fibroblast cultures by defined factors. Cell. 2006;126(4):663–76.
5. Yoshida Y, Yamanaka S. iPS cells: a source of cardiac regeneration. J Mol Cell Cardiol. 2011;50(2):327–32.
6. Bouwens L, Houbracken I, Mfopou JK. The use of stem cells for pancreatic regeneration in diabetes mellitus. Nat Rev Endocrinol. 2013;9(10):598–606.
7. Lancaster MA, Renner M, Martin CA, Wenzel D, Bicknell LS, Hurles ME, Homfray T, Penninger JM, Jackson AP, Knoblich JA. Cerebral organoids model human brain development and microcephaly. Nature. 2013;501(7467):373–9.
8. Hallett PJ, Deleidi M, Astradsson A, Smith GA, Cooper O, Osborn TM, Sundberg M, Moore MA, Perez-Torres E, Brownell AL, et al. Successful function of autologous iPSC-derived dopamine neurons following transplantation in a non-human primate model of Parkinson's disease. Cell Stem Cell. 2015;16(3):269–74.
9. Mungenast AE, Siegert S, Tsai LH. Modeling Alzheimer's disease with human induced pluripotent stem (iPS) cells. Mol Cell Neurosci. 2016;73:13–31.
10. Jungverdorben J, Till A, Brustle O. Induced pluripotent stem cell-based modeling of neurodegenerative diseases: a focus on autophagy. J Mol Med (Berl). 2017;95(7):705–18.
11. Ye L, Ni X, Zhao ZA, Lei W, Hu S. The Application of Induced Pluripotent Stem Cells in Cardiac Disease Modeling and Drug Testing. J Cardiovasc Transl Res. 2018;11(5):366–74.
12. Liu J, Han Q, Peng T, Peng M, Wei B, Li D, Wang X, Yu S, Yang J, Cao S, et al. The oncogene c-Jun impedes somatic cell reprogramming. Nat Cell Biol. 2015;17(7):856–67.
13. Hanna J, Saha K, Pando B, van Zon J, Lengner CJ, Creyghton MP, van Oudenaarden A, Jaenisch R. Direct cell reprogramming is a stochastic process amenable to acceleration. Nature. 2009;462(7273):595–601.

14. Peng L, Zhou Y, Xu W, Jiang M, Li H, Long M, Liu W, Liu J, Zhao X, Xiao Y. Generation of Stable Induced Pluripotent Stem-like Cells from Adult Zebra Fish Fibroblasts. Int J Biol Sci. 2019;15(11):2340–9.
15. Kogut I, McCarthy SM, Pavlova M, Astling DP, Chen X, Jakimenko A, Jones KL, Getahun A, Cambier JC, Pasmooij AMG, et al. High-efficiency RNA-based reprogramming of human primary fibroblasts. Nat Commun. 2018;9(1):745.
16. Huangfu D, Maehr R, Guo W, Eijkelenboom A, Snitow M, Chen AE, Melton DA. Induction of pluripotent stem cells by defined factors is greatly improved by small-molecule compounds. Nat Biotechnol. 2008;26(7):795–7.
17. Chin MH, Mason MJ, Xie W, Volinia S, Singer M, Peterson C, Ambartsumyan G, Aimiuwu O, Richter L, Zhang J, et al. Induced pluripotent stem cells and embryonic stem cells are distinguished by gene expression signatures. Cell Stem Cell. 2009;5(1):111–23.
18. Chen G, Guo Y, Li C, Li S, Wan X. Small Molecules that Promote Self-Renewal of Stem Cells and Somatic Cell Reprogramming. Stem Cell Rev Rep. 2020;16(3):511–23.
19. Broccoli V. Reprogramming of somatic cells: iPS and iN cells. Prog Brain Res. 2017;230:53–68.
20. Zhao T, Fu Y, Zhu J, Liu Y, Zhang Q, Yi Z, Chen S, Jiao Z, Xu X, Xu J, et al. Single-Cell RNA-Seq Reveals Dynamic Early Embryonic-like Programs during Chemical Reprogramming. Cell Stem Cell. 2018;23(1):31–45 e37.
21. Han JY, Han YK, Park GY, Kim SD, Lee CG. Bub1 is required for maintaining cancer stem cells in breast cancer cell lines. Sci Rep. 2015;5:15993.
22. Li SS, Liu YH, Tseng CN, Chung TL, Lee TY, Singh S. Characterization and gene expression profiling of five new human embryonic stem cell lines derived in Taiwan. Stem Cells Dev. 2006;15(4):532–55.
23. Wang Y, Fu Y, Yan Z, Zhang XB, Pei M. Impact of Fibronectin Knockout on Proliferation and Differentiation of Human Infrapatellar Fat Pad-Derived Stem Cells. Front Bioeng Biotechnol. 2019;7:321.
24. Bridges JP, Sudha P, Lipps D, Wagner A, Guo M, Du Y, Brown K, Filuta A, Kitzmiller J, Stockman C, et al. Glucocorticoid regulates mesenchymal cell differentiation required for perinatal lung morphogenesis and function. Am J Physiol Lung Cell Mol Physiol. 2020;319(2):L239–55.
25. Neganova I, Tilgner K, Buskin A, Paraskevopoulou I, Atkinson SP, Peberdy D, Passos JF, Lako M. CDK1 plays an important role in the maintenance of pluripotency and genomic stability in human pluripotent stem cells. Cell Death Dis. 2014;5:e1508.
26. Wang XQ, Lo CM, Chen L, Ngan ES, Xu A, Poon RY. CDK1-PDK1-PI3K/Akt signaling pathway regulates embryonic and induced pluripotency. Cell Death Differ. 2017;24(1):38–48.
27. Brill LM, Xiong W, Lee KB, Ficarro SB, Crain A, Xu Y, Terskikh A, Snyder EY, Ding S. Phosphoproteomic analysis of human embryonic stem cells. Cell Stem Cell. 2009;5(2):204–13.
28. Wang L, Schulz TC, Sherrer ES, Dauphin DS, Shin S, Nelson AM, Ware CB, Zhan M, Song CZ, Chen X, et al. Self-renewal of human embryonic stem cells requires insulin-like growth factor-1 receptor and ERBB2 receptor signaling. Blood. 2007;110(12):4111–9.

29. Hashimoto H, Wang Z, Garry GA, Malladi VS, Botten GA, Ye W, Zhou H, Osterwalder M, Dickel DE, Visel A, et al. Cardiac Reprogramming Factors Synergistically Activate Genome-wide Cardiogenic Stage-Specific Enhancers. Cell Stem Cell. 2019;25(1):69–86 e65.
30. Soyombo AA, Wu Y, Kolski L, Rios JJ, Rakheja D, Chen A, Kehler J, Hampel H, Coughran A, Ross TS. Analysis of induced pluripotent stem cells from a BRCA1 mutant family. Stem Cell Reports. 2013;1(4):336–49.
31. Penalosa-Ruiz G, Bousgouni V, Gerlach JP, Waarlo S, van de Ven JV, Veenstra TE, Silva JCR, van Heeringen SJ, Bakal C, Mulder KW, Veenstra GJC. WDR5, BRCA1, and BARD1 Co-regulate the DNA Damage Response and Modulate the Mesenchymal-to-Epithelial Transition during Early Reprogramming. Stem Cell Reports. 2019;12(4):743–56.

Tables

Tables are not available with this version.

Figures

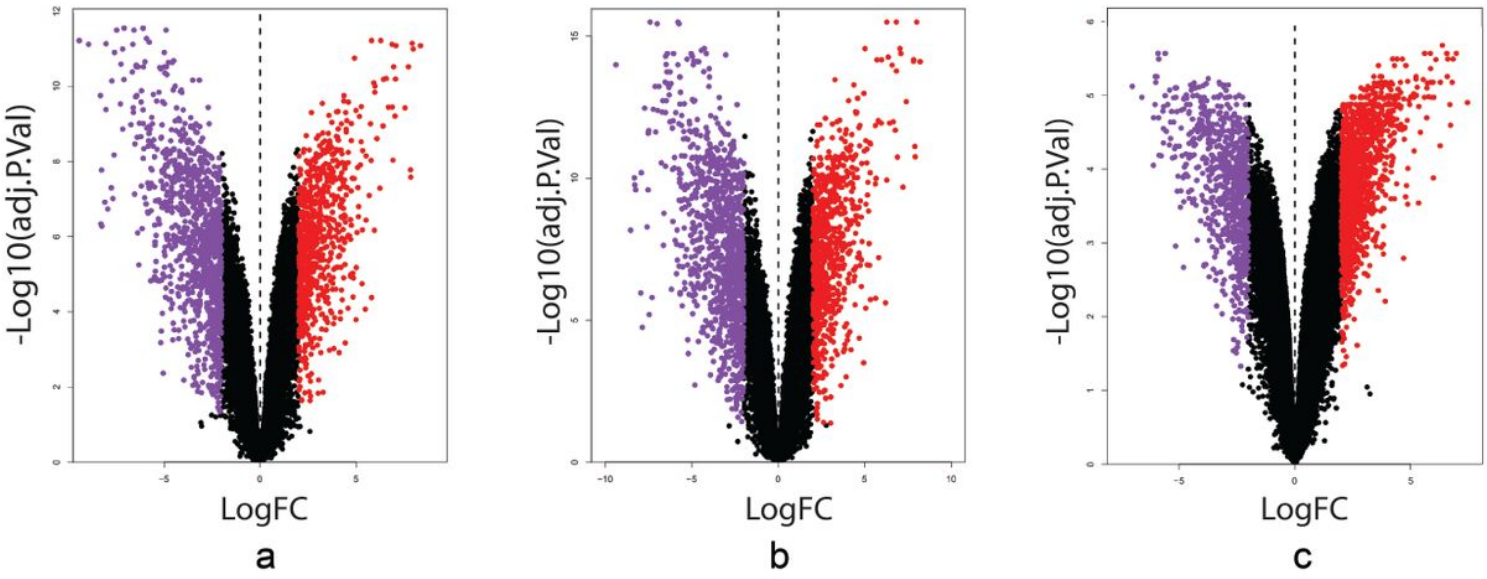

Figure 1

Volcano plot of gene expression profile data in FBs samples and hiPSCs ones: (a) volcano plot of GSE34309, (b) volcano plot of GSE43996, and (c) volcano plot of GSE86805. The red, purple, and black points represent up regulated genes, down regulated genes, and non-differentially expressed genes. They are screened based on |logFC|≥2.0 and adj. P□0.05.

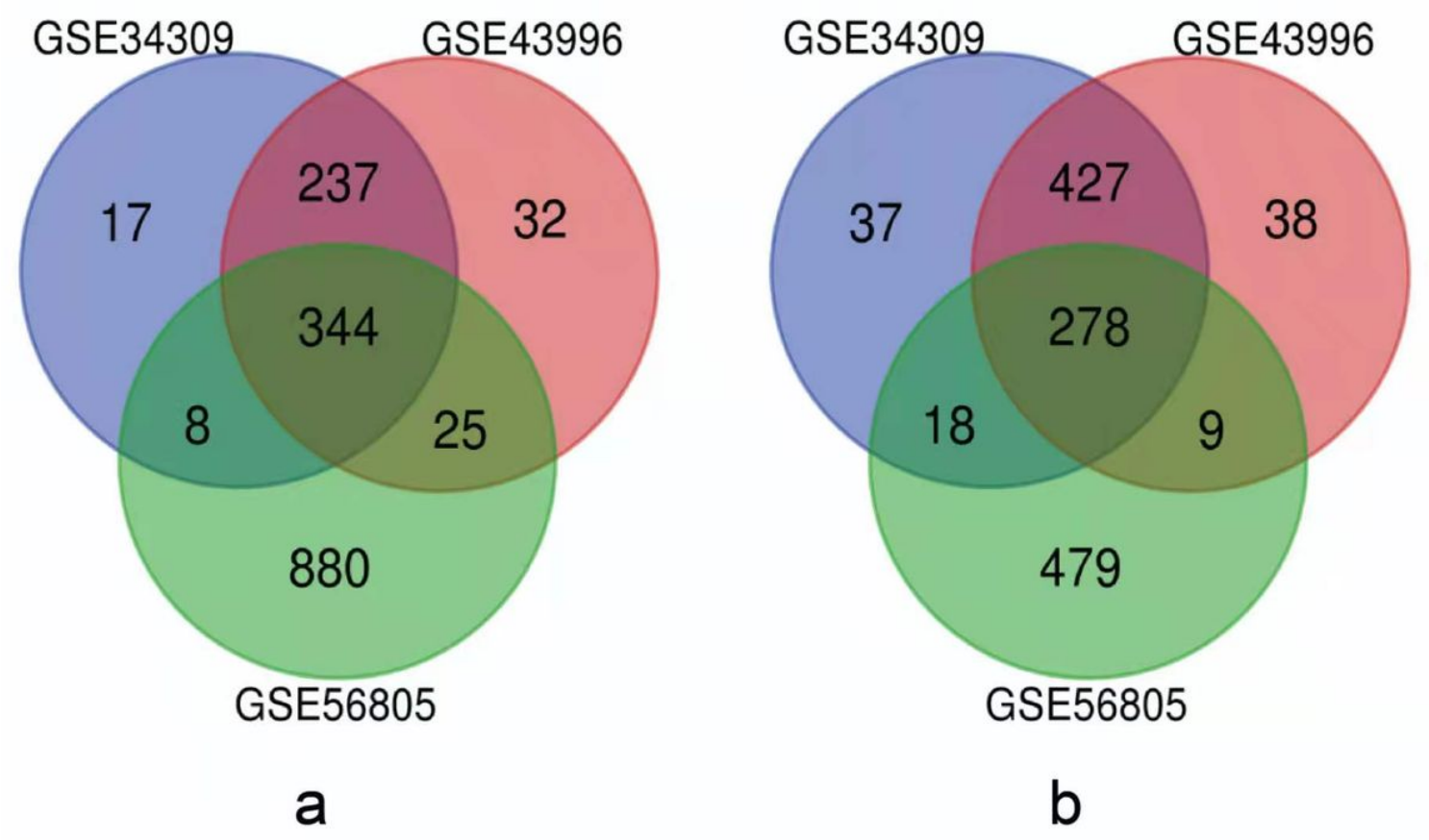

Figure 2

Venn diagram of DEGs common to all three GEO datasets: (a) up regulated genes, (b) down regulated genes.

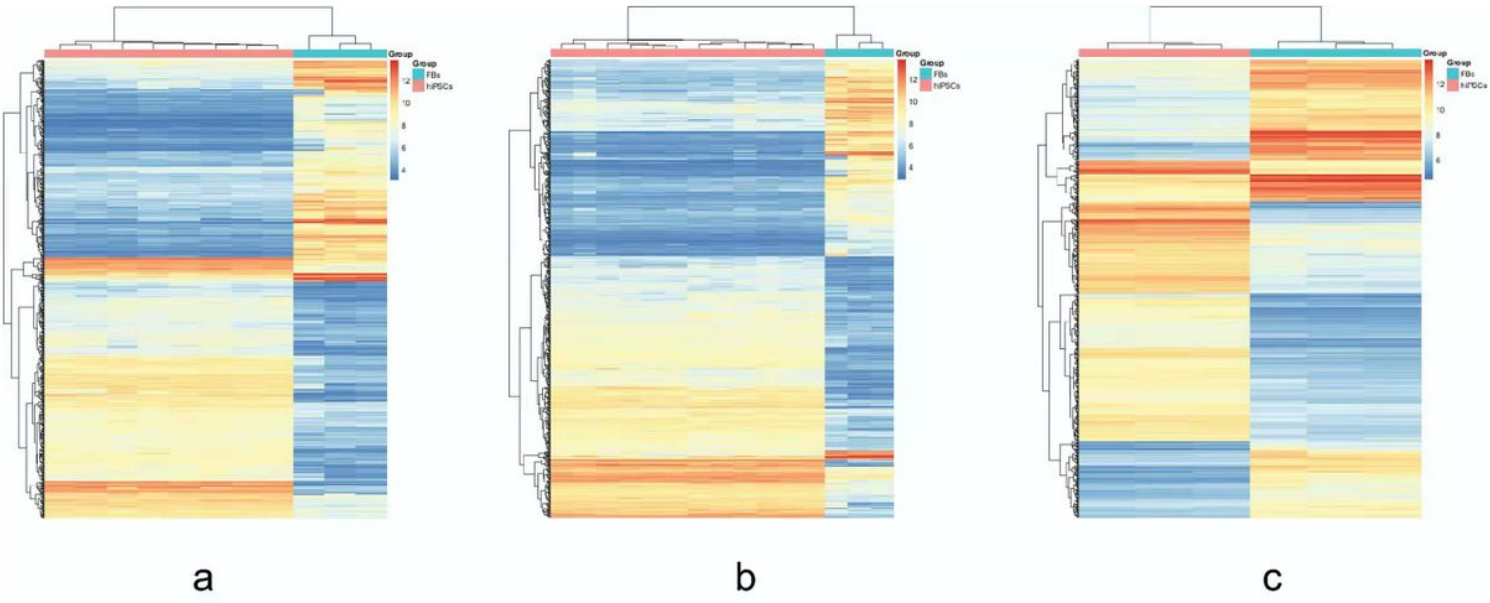

Figure 3

Hierarchical clustering heat map of DEGs, which was screened based on |logFC|≥2.0 and adj. P□0.05 :(a) GSE34309 data, (b) GSE43996 data, and (c) GSE56805 data. Red represents that the expression of genes

is relatively up regulated. Blue represents that the expression of genes is relatively down regulated.

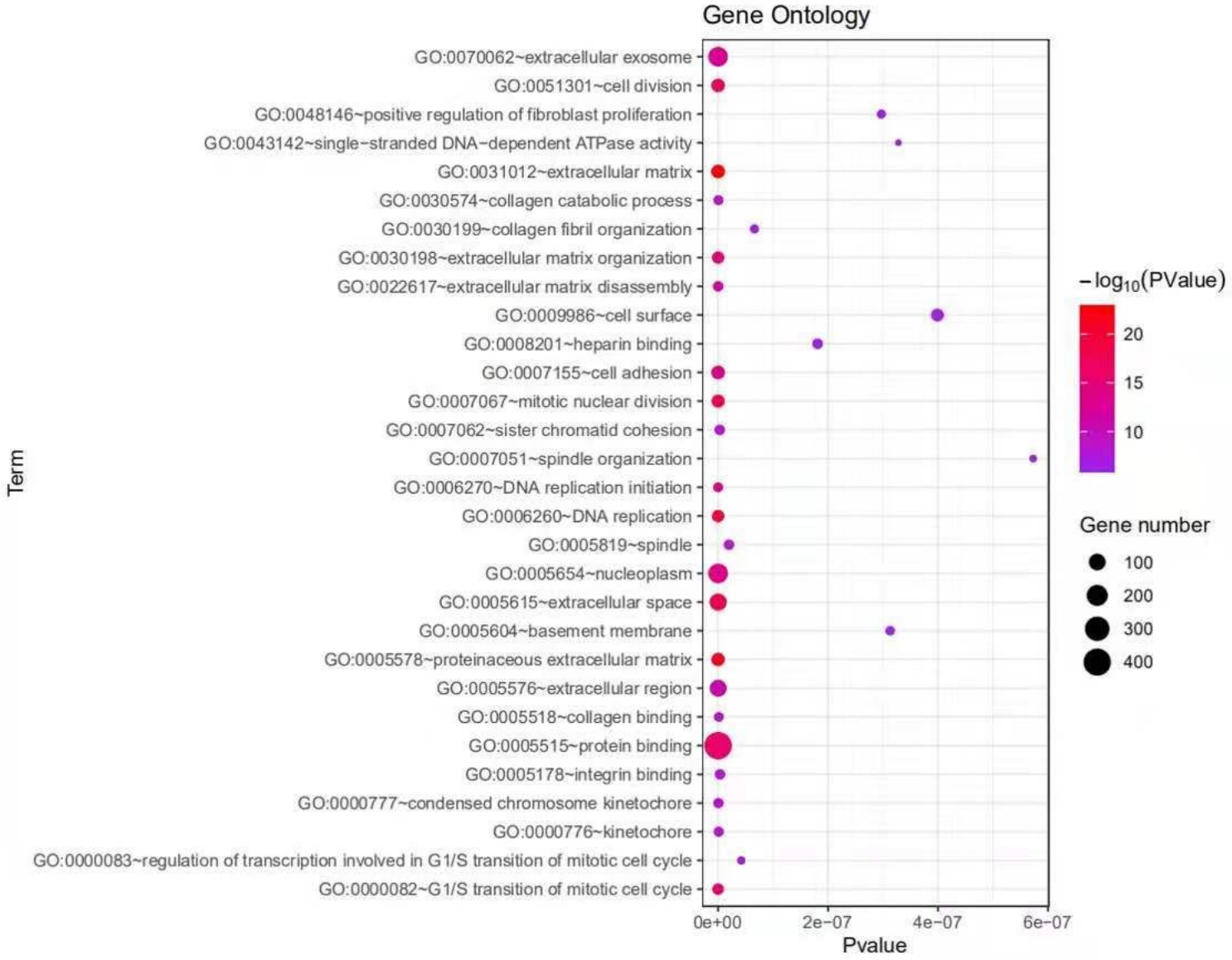

Figure 4

GO functional annotation analysis of DEGs: X-axis indicates P-value, Y-axis represents different functional groups (also named different GO terms). The dot size indicates the number of genes in different functional groups, and the color of the dot reflects the different -log(P-value) range. The bigger the gene count, the bigger the dot size is. The gradual color ranged from purple to red represents the changing process of -log(P-value) from small to big value.

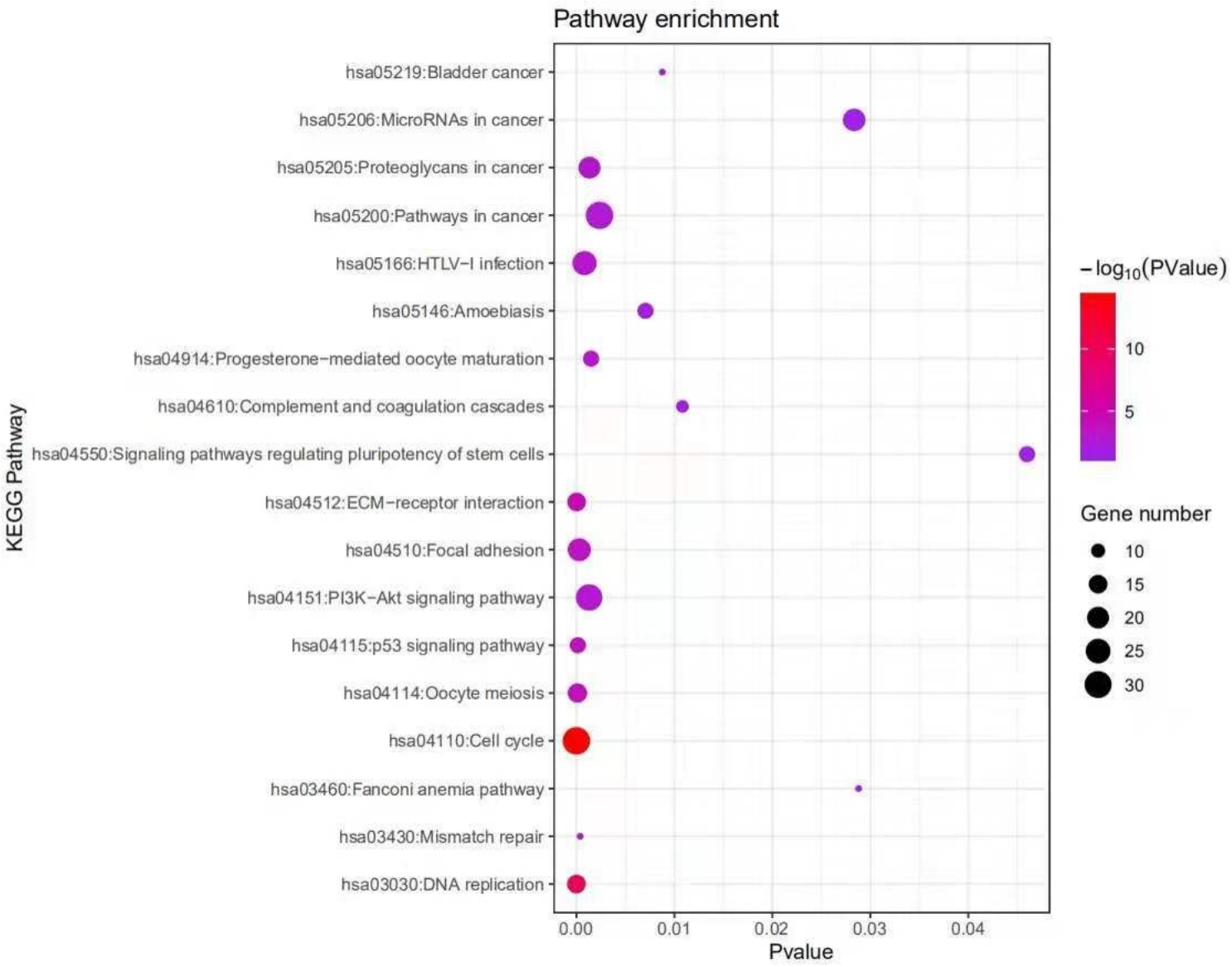

Figure 5

KEGG pathway enrichment analysis of DEGs: The X-axis indicates P-value, Y-axis represents different functional groups (also named different GO terms). The dot size indicates the number of genes in different functional groups, and the color of the dot reflects the different -log(P-value) range. The bigger the gene count, the bigger the dot size is. The gradual color ranged from purple to red represents the changing process of -log(P-value) from small to big value.

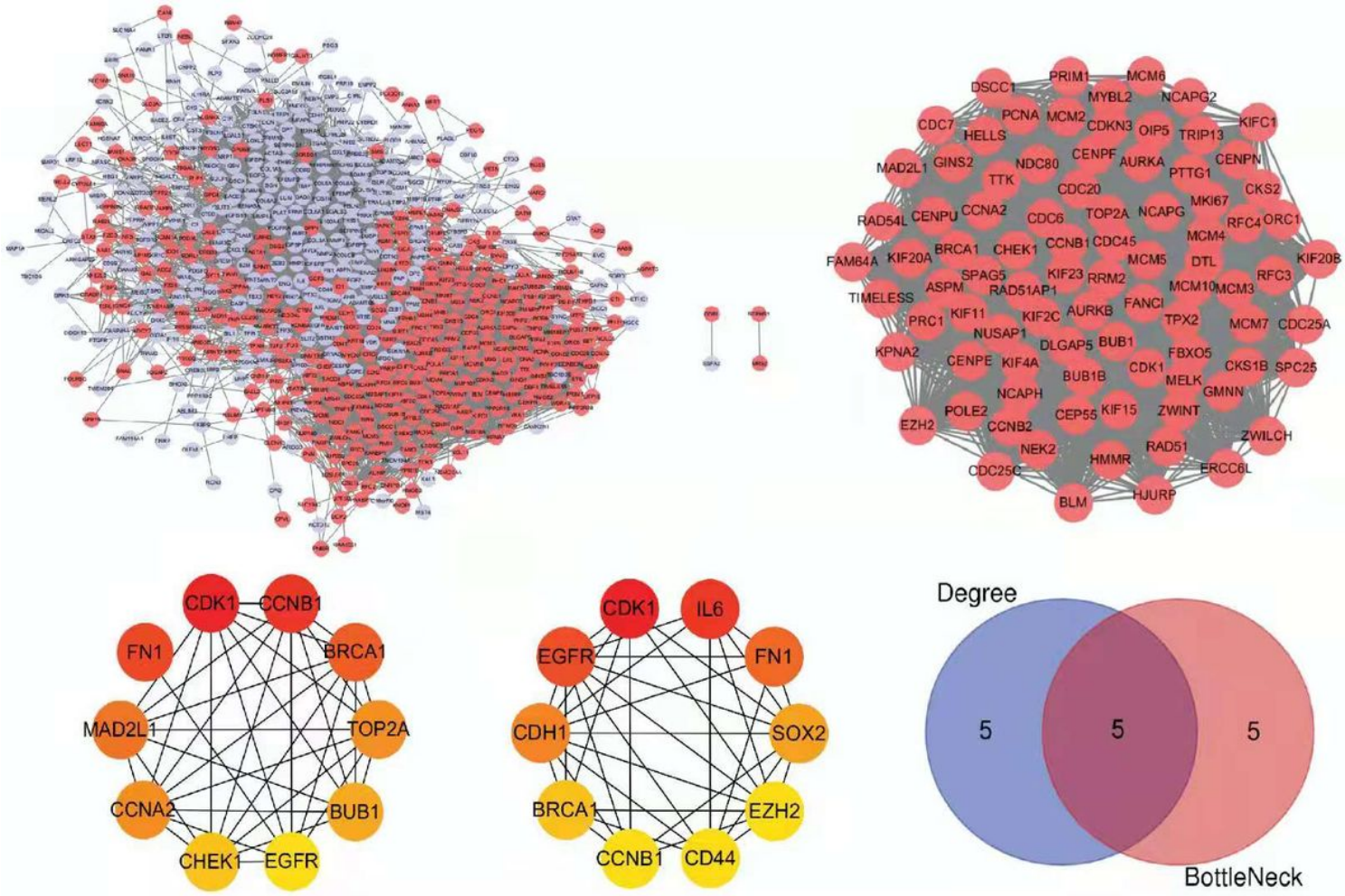

Figure 6

Establishment of PPI network, modules analysis, top 10 hub genes, and Venn diagram: (a) Whole PPI network. Circles and lines represent genes and the interaction of proteins between genes, respectively. The red represents the up regulated genes; the purple represents the down regulated genes. (b) PPI network of the module. Circles and lines represent genes and the interaction of proteins between genes, respectively. The red represents the up regulated genes. (c) Top 10 hub genes based on degree and (d) Bottleneck, (e) Venn diagram of mutual hub genes based on two methods.